

# A Study of the Jetting Evolution of NanoCopper Ink and NanoSilver Ink with Inkjet

Sooman Lim, Paul D. Fleming<sup>▲</sup>, and Margaret Joyce

Department of Chemical and Paper Engineering Western Michigan University, 4601 Campus Dr. # A-217

E-mail: sooman.lim@gmail.com

**Abstract.** The drop-on-demand inkjet is considered an important device for micro-electro-mechanical system production. Difficulties in understanding the fluid dynamic behavior of inks during drop ejection have led to the use of numerical simulations to predict drop formation. In this study, simulations were performed to predict and understand the jetting evolution of a nanocopper ink and a nanosilver ink. In order to predict the inkjetability of these inks, the Z number (the reciprocal of the Ohnesorge number) for different temperatures was determined. The results from the simulation studies were compared to experimental results obtained using a Dimatix inkjet printer. © 2013 Society for Imaging Science and Technology.

[DOI: 10.2352/J.ImagingSci.Technol.2013.57.2.020506]

## INTRODUCTION

Recently, as alternatives to conventional roll-to-roll contact printing methods, which require higher levels of process development to overcome the challenges of contact printing at high speeds, various alternative non-contact print methods, especially suitable for micropatterning, have been investigated.<sup>1</sup> Among those being investigated and used is inkjet printing, which has gained acceptance because it does not require a mechanical image carrier, can deposit various materials, and is environmentally friendly.<sup>2,3</sup> Inkjet technology has been a part of micro-electro-mechanical system (MEMS) processing for a long time. Not only are inkjet heads examples of MEMS devices, but they also can be used for printing MEMS devices.<sup>4,5</sup> For these applications, the ejection of fine drops has been well researched.<sup>6</sup> Thermal and piezoelectric actuation methods are commercially successful technologies among microdrop jetting techniques. However, since thermal action may cause changes in the material properties of a conductive nanoparticle ink, piezoelectric inkjet (PIJ) technology is preferred for the industrial printing of MEMS<sup>7</sup> and other printed electronics. Piezo drop-on-demand (DOD) inkjet printers are based on the piezoelectric effect. Drops are generated by mechanical displacement brought about by a digital image signal (waveform) sent to the piezo head contained in the ink chamber.

Many researchers have studied the fluid dynamics of drop-on-demand jets with numerical methods.<sup>8,9</sup> Fakhfour et al.<sup>10</sup> addressed the propagation of the pressure wave

along the capillary tube and the conversion of the kinetic energy of the liquid jet into surface energy being the main phenomena governing the process of piezo-type inkjets. Both phenomena can be characterized by dimensionless numbers, namely the Ohnesorge number ( $Oh$ )<sup>10</sup> and the Weber number ( $We$ ).<sup>10</sup> With these numbers, the possibility for droplet ejection and the forming of free satellites are estimated. In regards to generating a droplet, the calculation of these two dimensionless numbers is required to estimate whether proper drop ejection will occur. For proper drop ejection, first, the inertial forces at the orifice of the nozzles must be higher than the surface tension forces of the inks. This corresponds to the definition of  $We$ , which, as shown by Eq. (1), is the inertial force divided by the surface tension force acting on a fluid.<sup>11</sup>

$$We = \text{Inertial force/Surface tension force} \\ = d \cdot v^2 \cdot \rho \cdot \sigma^{-1}, \quad (1)$$

where  $d$  is the droplet diameter,  $v$  is its velocity,  $\rho$  is the liquid density, and  $\sigma$  is the surface tension of the liquid. For proper drop ejection, the inertial force should be higher than the surface tension force. Another important rheological dimensionless group is the Reynolds number (Eq. (2)),  $Re$ , which is defined as the kinetic energy divided by the viscous dissipation energy.

$$Re = d \cdot v \cdot \rho \cdot \eta^{-1}, \quad (2)$$

where  $\eta$  is the dynamic viscosity of the liquid. For simplicity, these two numbers are combined into one dimensionless number, the Ohnesorge<sup>10</sup> number:

$$Oh = \sqrt{We/Re} = \eta \cdot (\rho \cdot \sigma \cdot d)^{-0.5}. \quad (3)$$

The Z number is defined as the reciprocal of the  $Oh$  number:<sup>10</sup>

$$Z = (\rho \cdot \sigma \cdot d)^{0.5} / \eta = Oh^{-1}. \quad (4)$$

The Z number, introduced by Fromm,<sup>8</sup> is equally valid for characterizing jetting, providing a valid range for the drop formation to occur. Later, Reis et al.<sup>12</sup> reported that the prediction of ink ejection for concentrated alumina wax suspensions was in the range  $1 < Z < 10$  for a DOD inkjet printing system. At  $Z = 10$  or higher, satellite drops are formed. In addition, it was demonstrated that the relation

<sup>▲</sup> IS&T Member.

Received Oct. 28, 2011; accepted for publication May 20, 2013; published online Mar. 1, 2013. Associate Editor: Michael Lee.

1062-3701/2013/57(2)/020506/8/\$20.00

between the  $Z$  number and the drop volume is a proportional one. In regards to the  $We$  number, Pilch et al.<sup>13</sup> reported that there is no breakup when the  $We$  number is smaller than its  $We_{critical}$  (Eq. (5)),

$$We_{critical} = 12 \cdot (1 + 1.077 \cdot Oh^{1.6}). \quad (5)$$

Thus, the required velocity for ejection of ink at the inkjet head can be calculated.

For many printed electronics applications, silver ink is used, due to its high conductivity and solubility properties in many solvents. However, its high price has led to interest in the formulation and development of solution-processable copper inks for printing. New developments in copper ink technology have resulted in the commercial availability of copper-based inks, which can be applied by either screen or piezo-type inkjet print methods. Although both copper and silver inks have gained widespread use as conductive inks in the field of printed electronics, simulation studies comparing the drop ejection of nanocopper ink and nanosilver ink to experimental ink jetting results have not yet been reported. Tsai et al.<sup>14</sup> studied piezo inkjet printing of a silver nanopowder suspension. In particular, they investigated the effect of waveform amplitude (voltage) on jetting, but did not provide any numerical interpretation with flow simulations.

In this study, the drop formation of nanocopper (CI-002, Intrinsiq, CA) and nanosilver ink (TEC-IJ-010, InkTec, Korea), where, according to the manufacturer, all silver occurs in a soluble cluster complex in the solvent, was simulated. The results were compared with experiments performed using a laboratory-scale piezo-type inkjet printer (Dimatix Materials Printer DMP-2800, Fujifilm). From the ejection mechanism of the ink, the relationships between fluid flow, droplet formation, ejection pressure, and motion of the PZT (lead zirconate titanate, a piezoelectric material) element, were determined, based upon analyzing the  $Z$  number and  $We_{critical}$ . *FLOW-3D*, commercial simulation software, was used as the simulation tool, because it is a suitable software package for simulating drop formation processes and printing issues in various engineering applications.<sup>15–20</sup> These cited works fall into two categories. One category involves using commercial software to simulate flow of inks from orifices<sup>16,17</sup> or cells,<sup>15,18</sup> while the other involves improved numerical method development.<sup>8,9,19,20</sup> The work presented here falls into the former category. The latter is also of great interest to us in terms of improved convergence, numerical efficiency, and greater accuracy, which will expand the scale of problems that can be tackled with finite computational resources. However, such investigations are beyond the scope of the present work.

As a result of Fromm's<sup>8</sup> observation that the  $Z$  number nondimensionalizes the governing equations, every simulation run at a given  $Z$  number applies to a family of liquids with the same  $Z$  number. Thus, an optimum waveform (pressure/voltage pulses versus time) can be determined for a family of liquids. This is nontrivial, because, as we will

see later, different fluids with different  $Z$  number require different waveforms.

## EXPERIMENT

### Dimensional analysis

A commercial nanocopper ink containing 25 nm diameter particles (10% wt, as reported by the supplier) uniformly dispersed in a mixture of ethane-1,2-diol and n-butanol and a nanosilver ink, containing nanosilver cluster complexes dissolved in alkyl amine, were used. In order to predict the inkjetability of the nanocopper ink and nanosilver ink, the  $Z$  numbers for the inks were determined at different temperatures. Since the  $Z$  number is a function of temperature, changes in cartridge temperature during the printing process had to be considered. The surface tension with various temperatures was measured using a First Ten Angstrom FTA 200 surface tension analyzer by the pendent drop method. A syringe heater (Newera, NY) was wrapped on the syringe containing each ink to increase the temperature of the ink, enabling the measurement of surface tensions over a temperature range from 25 to 70°C. For the viscosity, the steady-state flow method was conducted for the same range of temperature that was applied to the surface tension measurement using an RA 2000 viscometer in which the shear rate was fixed at 10 s<sup>-1</sup>. This shear rate was determined to be in the second linear region of the steady flow curve. The theoretical minimum velocity required for generating drop ejection at print heads was estimated by the dimensional analysis of  $We_{critical}$ .

### Numerical approaches

*FLOW-3D* (Ver. 9.3, Flow science), commercial software for engineers, was used to solve the numerical equations for simulating ink ejection from the nozzle of the DMP printer. The ink was assumed to be incompressible and homogeneous. Negligible gravity effects were also assumed, meaning that the Bond number<sup>22</sup>  $\ll 1$  or the surface tension is dominant. The Bond number is given by  $Bo = \rho g a^2 / \gamma$ , where  $\rho$  is the liquid density,  $\gamma$  is the surface tension of the fluid,  $g$  is the acceleration due to gravity, and  $a$  is the drop diameter. In this case, typical properties of fluid used for inkjet printing were substituted, such as 1 g cm<sup>-3</sup> for density, 100  $\mu$ m for drop diameter, and 29 dyne/cm for the surface tension, resulting in a  $Bo$  number of 0.0033. Non-Newtonian flow was also assumed, with a sharply defined free surface being assumed present during simulation. The governing equations applied are the Navier–Stokes equation and continuity equations:<sup>21</sup>

$$\rho \frac{D\vec{V}}{D\tau} = \rho \vec{g} - \nabla^2 \vec{V}, \quad (6)$$

$$\nabla \cdot \vec{V} = 0. \quad (7)$$

where  $\vec{V} = (u, v, w)$  is the velocity vector,  $\rho$  is the mass density,  $\vec{g}$  is the acceleration due to gravity,  $p$  is the pressure,  $\eta$  is the shear viscosity of the fluid, and  $\tau$  is a time variable. In



Figure 1. Illustration of the inkjet head design created using FLOW-3D.

Figure 1, for this problem, only half of the ink jet geometry was modeled to reduce the computational time, because there is the symmetry plane on the left boundary. The top boundary (+ $z$  direction) was a continuative boundary through which the outflow occurred. The bottom boundary ( $-z$  direction) was a specified pressure applied as a function of time. For cylindrical coordinate problems, the mesh is defined in terms of cylindrical coordinates. An initial maximum time step was set for this case as 100  $\mu\text{s}$ . The nozzle is a toroid with a concave inner edge. In Fig. 1, an illustration of the inkjet head design created using *FLOW-3D* is shown.

The total ejection length from the nozzle ( $z$  direction) used in the simulation was 500  $\mu\text{m}$  and the diameter of the nozzle orifice used was 21.5  $\mu\text{m}$ , which is the orifice size of the DMP printer.

Figure 2 shows the two-dimensional (2D) modeling ( $x$ ,  $z$  cross sections) designed using *FLOW-3D* software with the nozzle diameter corresponding to the diameter of the nozzle of the DMP printer. A long channel ink chamber with a nozzle configuration, as shown Fig. 2, is the basic geometry used for the inkjet head.

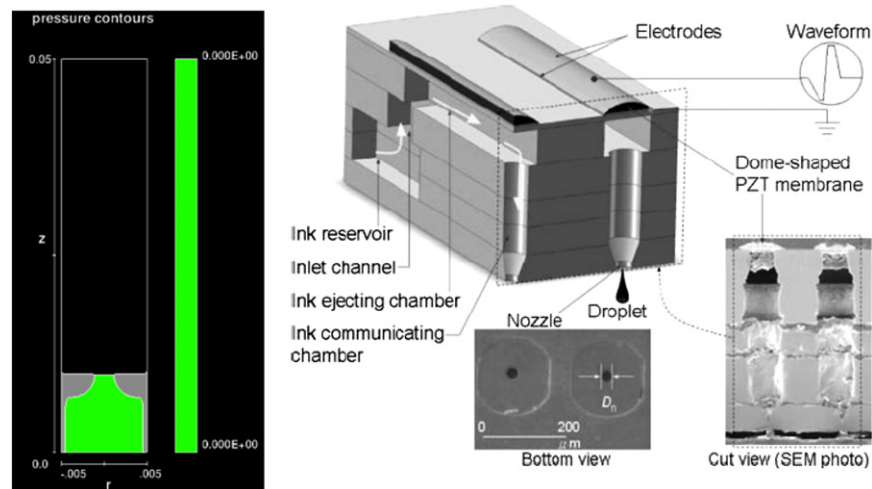


Figure 2. 2D piezo inkjetting modeling in accordance with the DMP printer used in this experiment (left, by *FLOW-3D*) and the structural, bottom, and cut views of the PIJ printhead.<sup>22</sup>

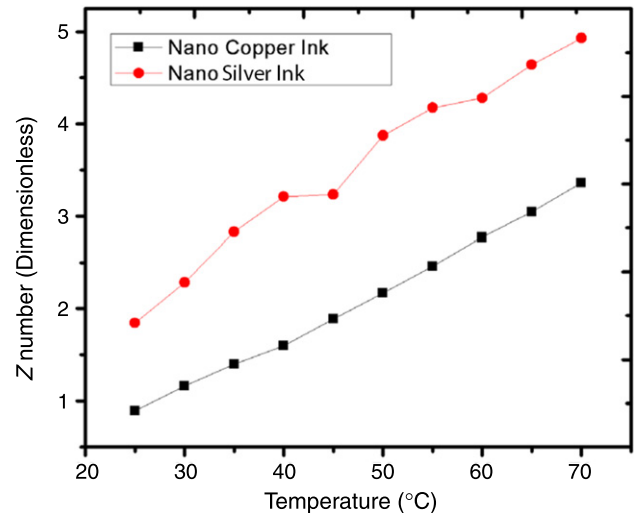


Figure 3. Influence of temperature on the calculated Z number for the nanocopper ink and nanosilver inks.

In order to compare the simulation results with experimental data, the drop evolution progress was recorded using the drop watcher camera (installed on the DMP printer) for 100  $\mu\text{s}$ . With the recorded images, simulations were performed to determine the set-up parameters in the software required to match the experimental results. Specifically, step changes to the applied pressure, which were negative and positive, were followed by waveform adjustments being made. In addition, the change in meniscus in the nozzle with time was simulated. Besides, the evolution of drop formation was depicted clearly with the visualized simulation results.

## RESULTS AND DISCUSSION

### Dimensional analysis

Figure 3 shows the Z numbers for the nanocopper ink and nanosilver ink at different temperatures calculated according

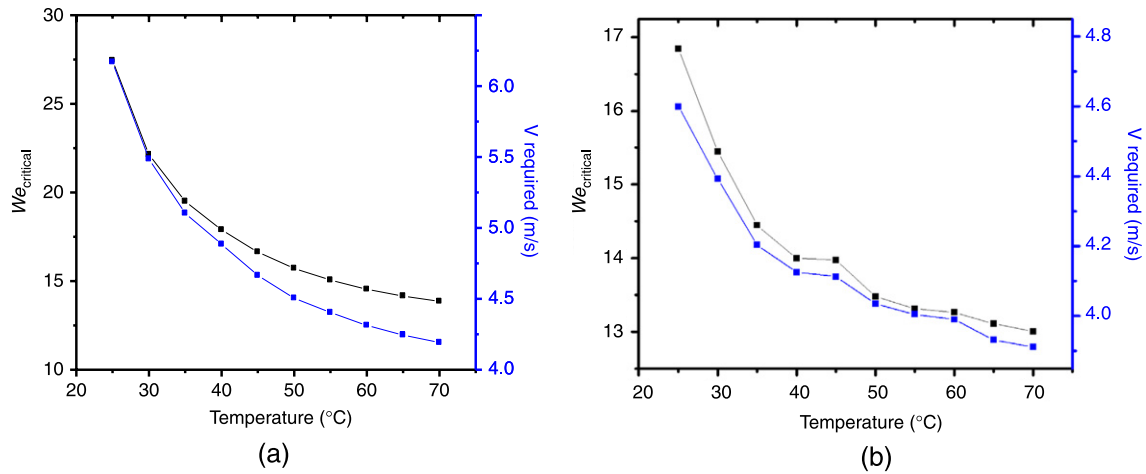


Figure 4. Influence of temperature on the  $We_{critical}$  and minimum drop speed for nanocopper (a) and nanosilver inks (b).

to Eqs. (3) and (4) in which a density of  $1.0 \text{ g cm}^{-3}$  and the droplet diameter of  $21.5 \mu\text{m}$  corresponding to the nozzle diameter was used.

The surface tension and viscosity change with temperature; in particular, both of these properties decrease as the temperature is raised. The range of  $Z$  number was  $0.89 < Z < 4.5$  for nanocopper ink and  $1.84 < Z < 4.92$  for nanosilver ink in the temperature range measured, respectively, as shown in Fig. 3. Thus, jetting of the nanocopper was predicted to be possible above  $25^\circ\text{C}$  and the nanosilver ink was predicted to be jettable at  $25^\circ\text{C}$  and above.

The reason for the different jetting temperature expected for each ink was attributed to the  $Z$  values calculated at experimented temperature where the value should be greater than 1 for proper jetting performance as described above. This, indeed, was found experimentally. The reason why the  $Z$  number for nanosilver ink has a higher value at the same temperature is due to its smaller particle size and solvent characteristics. For the solvents, especially, the alkyl amine used in the nanosilver ink has a lower boiling point than the glycerol used in the nanocopper ink, resulting in much more sensitivity to changes of temperature, thereby affecting the viscosity.

In Figure 4, the required drop velocity for jetting both of the inks was calculated, using Eq. (1) according to the result of  $We_{critical}$  obtained from Eq. (5). The calculated minimum velocity was 4.19 and 3.91 m/s at the temperature of  $70^\circ\text{C}$  and rose to 6.1 and 4.59 m/s when the temperature was reduced to  $25^\circ\text{C}$  for nanocopper ink and nanosilver ink, respectively. This change in minimum drop velocity required for jetting was caused by the increase in minimum kinetic energy required for drop formation to overcome the stronger intermolecular forces between ink components at the lower temperature.

To validate these predictions experimentally, drop ejection at the various cartridge temperatures was recorded with fixed waveform and meniscus vacuum of 5.6 mm Hg. The conditions used were set based on the recommended standard values to achieve drop ejection for a Dimatix model fluid. The applied voltage was 40 V, the maximum

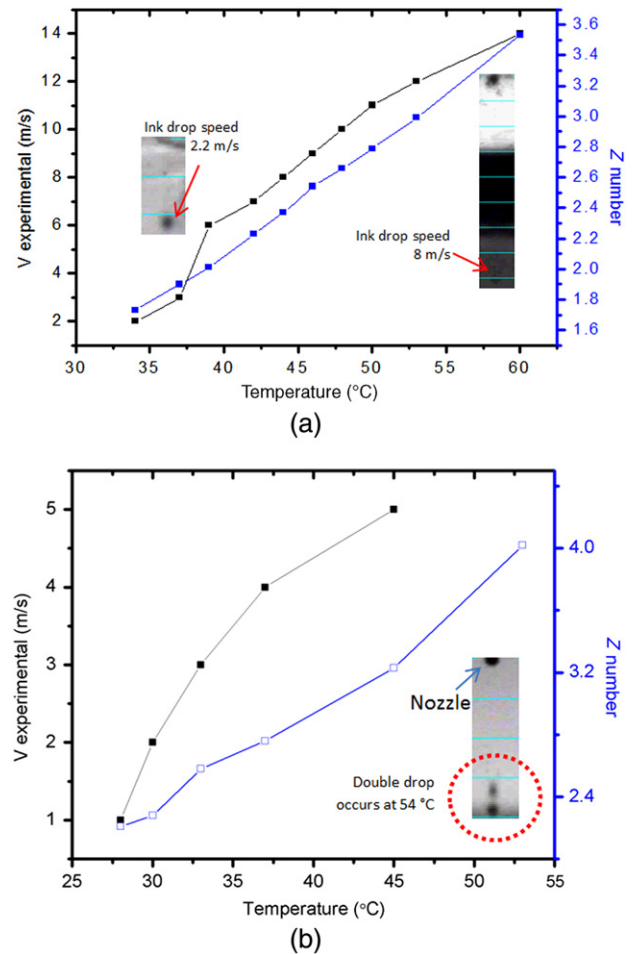


Figure 5. The result of drop ejection with temperature as compared to  $Z$  number for nanocopper (a) and nanosilver (b).

value the DMP printer can generate. For the nanocopper ink, jetting began at  $34^\circ\text{C}$  with a drop speed of 2.2 m/s (Figure 5(a)). This corresponds to a  $Z$  number of 1.16, which falls in the  $Z$  number range between 1 and 10. A similar result was found for the nanosilver ink, which required a  $Z$  number of 2.21. This  $Z$  number was achieved with a



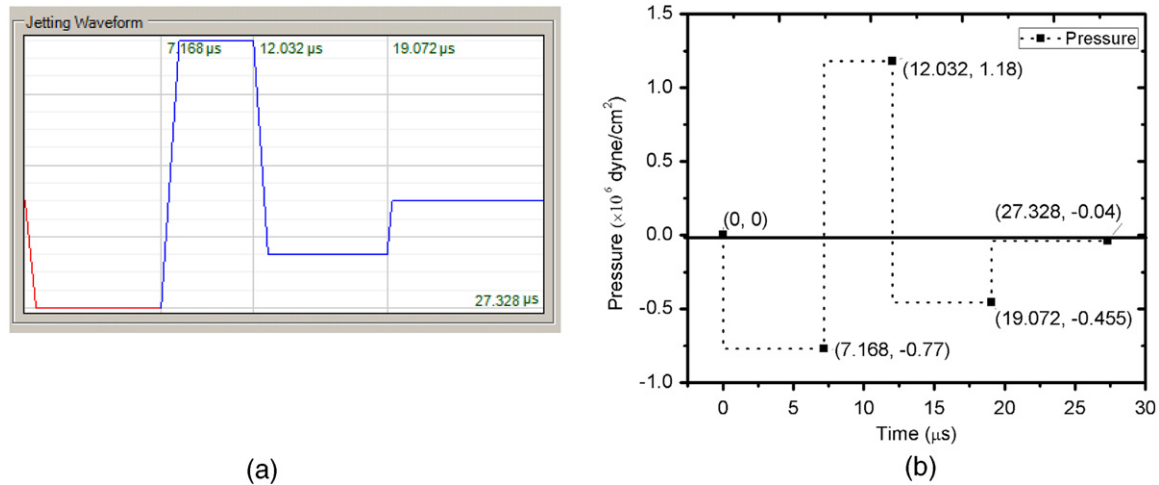


Figure 6. Experimentally applied jetting waveform (a) and simulated pressure in the ink chamber with time (b) for nanocopper ink.

drop speed of 1 m/s at 28°C and applied voltage of 40 V. It was also determined that both the jetting speed and Z number were proportional to the temperature applied, and that the size of the drops became finer as the drop speed was increased. The reason for the faster drop speed and smaller drop size with increasing temperature is the increase in  $We$  number and  $Re$  number caused by the fall in viscosity and surface tension.<sup>23</sup> In regards to this assumption, the double drop generated at 54°C for nanosilver ink can support this assumption in Fig. 5(b). First, the drop fired at the nozzle had a tail belonging to its main drop. Then, the satellite drop occurred when the drop reached to 400 μm long, because intermolecular action in the drop was weakened by the increased temperature, resulting in breaking of the drop.

### Simulation of jetting evolution

In order to determine the relationship between the waveform and the pressure generated from the waveform,<sup>24</sup> jetting evolution was simulated using *FLOW-3D*. For the nanocopper ink, the experimental data values input into the program were 1 g cm<sup>3</sup> for the density, 28.8 dyne/cm for the surface tension, and 18.3 cp for the viscosity at 34°C. Based on these factors, the drop speed was 2.2 m/s at a firing voltage of 40 V.

The applied waveform (Fig. 5(a)) shows the four time intervals classified with time as follows: first charging (up to 7.168 μs), discharging (up to 12.032 μs), second charging (up to 19.072 μs), and equilibration (up to 27.328 μs) with applied voltage (V). The first charging time interval is the negative displacement time zone of the PZT that draws fluid into the pumping chamber. Then, the firing pulse (positive displacement, discharging) is applied to the PZT, resulting in the ejection of the ink drop from the nozzle. As a final step to finish one cycle ejection, the PZT is going back to where it was. In addition to the displacement of the PZT, there are three main functions that are called level, slew rate, and duration to control the PZT displacement. Level indicates how far the piezomaterial is bent. Slew rate and duration show how fast the material is bent and how long it stays in that position, respectively. By adjusting these parameters,

the ink ejection can be controlled properly. In Figure 6, the up and down shape, tilting, and time indicate the level, slew rate, and duration, respectively. However, one thing to note is that there is no universal waveform suitable for both inks, even if the amplitude and timescales are rescaled, due to the variations in their physical and chemical properties.

In a piezo-type inkjet system, the pulse applied to the PZT generates a pressure wave inside the channel, leading to the ejection of the ink from the chamber. The resulting pressure for the waveform shown, as generated from the simulation software, is shown in Fig. 6(b). The pressure generated was obtained by applying various voltages with time. The agreement of these pressures with the experimental data was validated by comparing the drop velocity values with Figure 7 at a specific time.

Fig. 7 compares the evolution of a simulated and experimental ejected droplet captured using the drop watcher on the DMP printer.

During the time that the reverse pulse ( $-z$  direction pressure) was applied to the PZT for 7.168 μs in Fig. 6(b), the PZT was pulled up as much as during the applied pulse at 10.9 μs, which resulted in an increase in ink capacity because of the expanded ink chamber and pulling of the ink meniscus into the ink chamber. Since the PZT was originally pushed down toward the ink chamber, the first step should be to apply a negative voltage, causing it to retract. Then, the PZT was pushed down into the chamber for the time period allowed by the waveform from 7.168 to 12.03 μs, which led to the ejection of the ink from the nozzle at 13.98 μs. As the ink falls from the nozzle, the column of ejected ink forms a spherical droplet with a tail at 51.98 μs. In addition, the concave meniscus remained constant at the nozzle due to capillary action within the nozzle. Although the time of  $z$  direction pressure begins at 7.168 μs, the ejection does not occur simultaneously because the time for the transfer of the pressure waves through the ink is affected by the viscosity, surface tension, and density of the ink. At time 64.9 μs, the tail recoiled into the main droplet to form a complete droplet, because of the surface tension. Finally, the tail was reunited

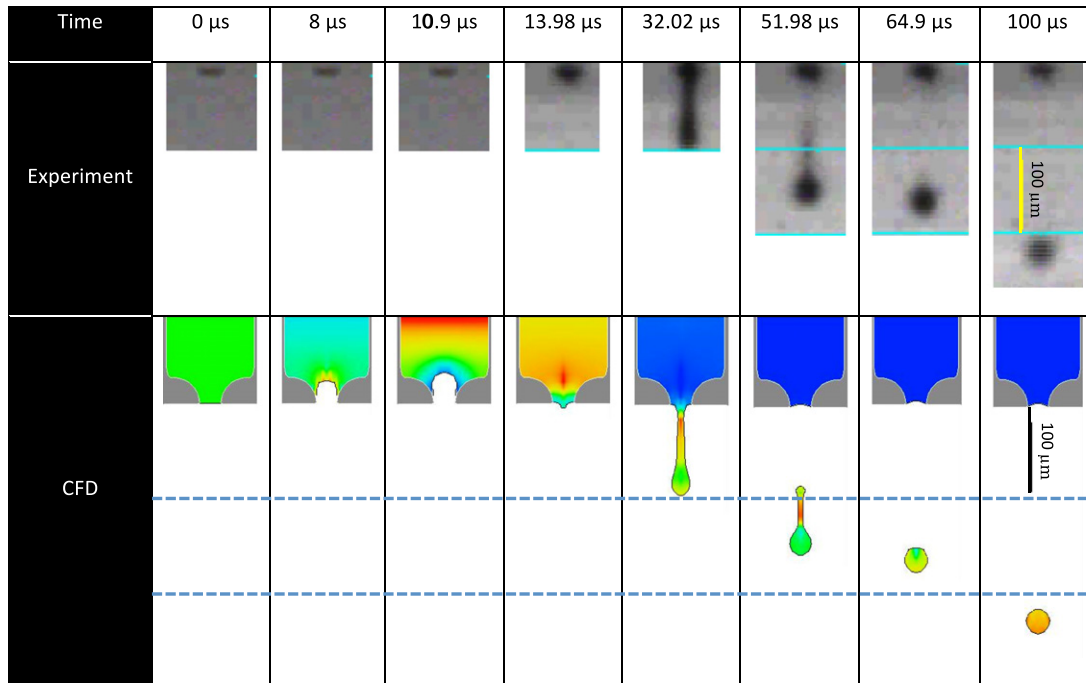


Figure 7. Comparison of drop evolution and drop ejection pictures obtained experimentally and using CFD (computational fluid dynamics) software for the nanocopper ink.

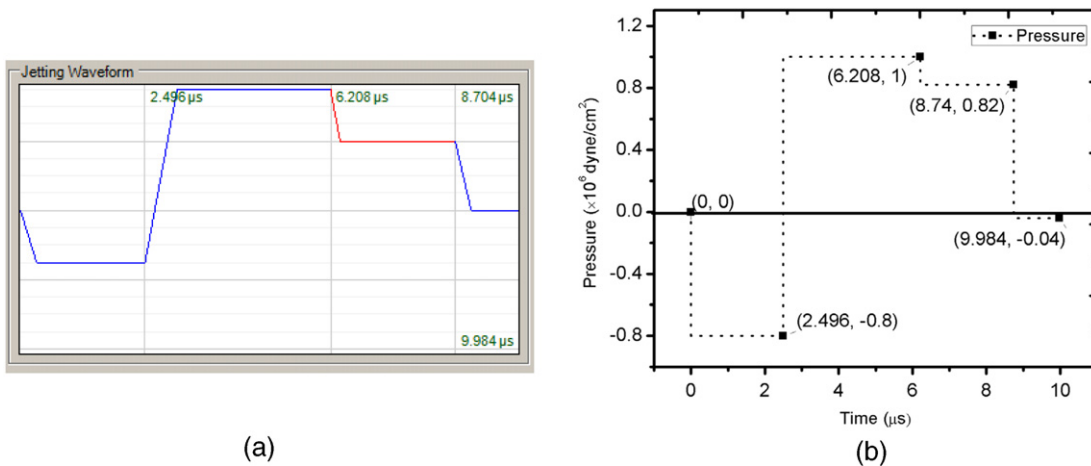


Figure 8. Experimentally applied jetting waveform (a) and simulated pressure in the ink chamber with time (b) for nanosilver ink.

with the main drop, where it proceeded in free flight before hitting the target at 100  $\mu\text{s}$ .

For nanosilver ink simulation, the values 1  $\text{g}/\text{cm}^3$  for density, 27.0  $\text{dyne}/\text{cm}$  for surface tension, and 11.5 cp for viscosity at 28°C were input to the program. Based on these factors, the drop speed for the jetting waveform was 1 m/s at a firing voltage of 40 V. This corresponds to the condition optimized to bring about an initial ejection from the nozzle like that for the nanocopper ink. The experimental waveform used is shown in Figure 8.

Unlike the waveform used in nanocopper ink, the applied waveform in Fig. 8(a) shows the four PZT displacement intervals classified with time as follows: first charging (up to 2.496  $\mu\text{s}$ ), discharging (up to 6.208  $\mu\text{s}$ ), second discharging (up to 8.704  $\mu\text{s}$ ), and equilibration (up to 9.984  $\mu\text{s}$ ) with

applied voltage. Since the viscosity of the nanosilver ink (11.5 cp) was lower than that of nanocopper ink (18.3 cp), less time was needed to make a drop, as shown in Fig. 8(b). Figure 9 shows the evolution of ink ejection with time for the nanosilver ink. At 7.98  $\mu\text{s}$ , a high pressure was applied into the chamber, resulting in ejecting the fluid out from the nozzle.

Figure 10 shows how the waveform applied on each ink impacts ink ejection. The waveforms used for each ink were exchanged and the results were compared to the experimental data. The other factors affecting jetting evolution on each ink, such as firing voltage, cartridge temperature, and meniscus vacuum, were fixed. The drop evolution simulation result for the nanosilver ink is compared in Fig. 10(a) to the experimental result obtained at the 4.39  $\mu\text{s}$  timing mark. The

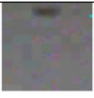
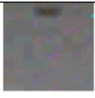
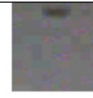
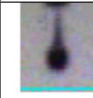




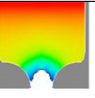
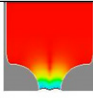
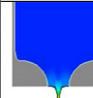
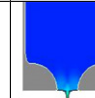
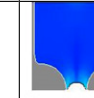
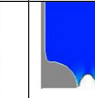
Time	0 $\mu\text{s}$	5.01 $\mu\text{s}$	7.98 $\mu\text{s}$	51.02 $\mu\text{s}$	53.98 $\mu\text{s}$	77.97 $\mu\text{s}$	100 $\mu\text{s}$
Experiment							
CFD							

Figure 9. The evolution of an ejected droplet (experiment compared with CFD) for nanosilver ink.

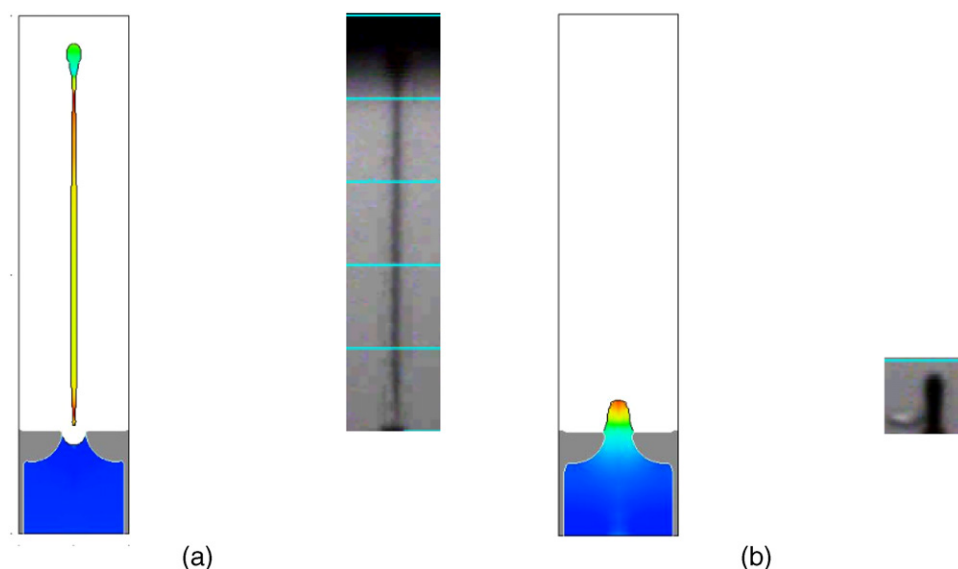


Figure 10. The comparison of simulation results with experimental data obtained by exchanging the waveforms used on each ink.

evolution of the nanocopper ink is compared, based on the waveform used for the nanosilver ink, at the 1.90  $\mu\text{s}$  timing mark in Fig. 10(b).

Although ink ejection occurred to some extent for the nanosilver ink with the use of the nanocopper waveform, in Fig. 10(a), a long tail tending to be a satellite drop remained during ink flight. For the nanocopper ink, there was no ink ejection but instead only a fluctuation in the ink, as shown in Fig. 10(b). Thus, it was verified that the waveform used for a specific ink does not produce the same jetting behavior as that when waveforms determined for other inks are used. Instead, a new waveform must often be determined for a given ink used. In addition, the simulation for the nanosilver ink was in good agreement with the experimental results, where there was about a 20  $\mu\text{m}$  extension error for the nanocopper ink, as shown in Fig. 10(b).

## CONCLUSIONS

In order to predict the inkjetability of nanocopper ink and nanosilver ink, the  $Z$  numbers calculated at different temperatures were determined. In addition to performing these calculations, a CFD simulation was performed. Based on these results, the  $Z$  number of nanosilver ink having lower viscosity than that of nanocopper ink fell in the proper range of  $Z$  number at room temperature, resulting in ink ejection taking place.

Thus, it is shown that the  $Z$  number not only provides a valid range for drop formation to occur, but also that it will be useful for formulating inks to fit the specific printing environment in terms of viscosity, surface tension, and density, and predicting jetting performance at certain temperatures. Moreover, the minimum velocity required to eject the drop out of the nozzle was theoretically calculated to predict the pressure that needs to be applied to the

nozzle. The relationship between the drop velocity and cartridge temperature was measured experimentally. On the other hand, the drop ejection shows good agreement with theoretical expectations simulated by commercially available software.

The results demonstrate the relationship between pressure and motion of a piezoelement based on the change in viscosity and surface tension. In that case, it required lower pressure (=lower voltage) and different waveform features for the nanosilver ink to make initial ejection compared to the nanocopper ink, due to its lower viscosity and surface tension, which is attributed to smaller particle size and lower boiling point. This was depicted clearly with the visualization of the simulation results.

## REFERENCES

- <sup>1</sup> R. Ohgashi and K. Tsuchiya, IEEE MEMS 2001, p. 389, (2001).
- <sup>2</sup> A. Rida, L. Yang, R. Vyas, and M. M., "Conductive inkjet-printed antennas on flexible low-cost paper-based substrates for RFID and WSN applications," *IEEE Antennas and Propagation Magazine* **51**, (2009).
- <sup>3</sup> S.-J. Park, W. Sim, Y. Yool, and J. Joung, 1-4244-0140-2/06, IEEE. (2006).
- <sup>4</sup> B. B. Narakathu, M. S. Devadas, A. S. G. Reddy, A. Eshkeiti, A. Moorthi, I. R. Fernando, B. Miller, G. Ramakrishna, E. Sinn, M. Joyce, M. Rebrosov, E. Rebrosova, G. Mezei, and M. Z. Atashbar, "Novel fully screen printed flexible electrochemical sensor for the investigation of electron transfer between thiol functionalized viologen and gold clusters," *Sensors and Actuators B: Chem.* **176**, 768–774 (2012).
- <sup>5</sup> A. S. G. Reddy, B. B. Narakathu, M. Z. Atashbar, M. Rebrosov, E. Hrehorova, B. J. Bazuin, M. K. Joyce, P. D. Fleming, and A. Pekarovicova, "Printed capacitive based humidity sensors on flexible substrates," *Sensor Lett.* **9**, 869–871 (2011).
- <sup>6</sup> F. Pan, J. Kubby, and J. Chen, Numerical simulation of fluid-structure interaction in a MEMS diaphragm drop ejector, IOP publishing Ltd, 0960-1317, (2002).
- <sup>7</sup> D. J. Hayes, W. R. Cox, and D. B. Wallace, "Printing System for MEMS Packaging," SPIE Con. on Micro and Microfab., p. 1. (2001).
- <sup>8</sup> J. E. Fromm, "Numerical calculation of the fluid dynamics of drop-on-demand jets," *IBM J. Res. Develop.* **28**, 322–333 (1984).
- <sup>9</sup> T. W. Shield, D. B. Bogy, and F. E. Talke, "Drop formation by DOD ink-jet nozzles: A comparison of experiment and numerical simulation," *IBM J. Res. Develop.* 96–110 (1987).
- <sup>10</sup> V. Fakhfour, G. Mermoud, J. Y. Kim, A. Martinoli, and J. Brugger, "Drop-on-demand inkjet printing of SU-8 polymer," *Micro and Nanosyst.* **1**, 63–67 (2009).
- <sup>11</sup> G. O. Thomas, "The aerodynamic breakup of ligaments," *Atomization Sprays* **13**, 117–129 (2003).
- <sup>12</sup> N. Reis, C. Ainsley, and B. Derby, "Ink-jet delivery of particle suspensions by piezoelectric droplet ejectors," *J. Appl. Phys.* **97**, (2005) 094903-6.
- <sup>13</sup> M. Pilch and C. A. Erdman, "Use of breakup time data and velocity history data to predict the maximum size of stable fragments for acceleration-induced breakup of a liquid-drop," *Int. J. Multiphase Flow* **13**, 741–757 (1987).
- <sup>14</sup> W. S. Mhtsai, H. H. Hwang, P. H. Chou, and P. H. Hsieh, "Effects of pulse voltage on inkjet printing of a silver nanopowder suspension," *Nanotechnology* **19**, 335304 (2008).
- <sup>15</sup> S. M. Lim, J. T. Youn, and K. H. Kim, "Computer simulation of ink flow in the conventional gravure cell," *J. Korea Printing Soc.* **25**, 109–120 (2007).
- <sup>16</sup> P. H. Chen, H. Y. Peng, H. Y. Liu, S. L. Chang, T. I. Wu, and C. H. Cheng, "Pressure response and droplet ejection of a piezoelectric inkjet printhead," *Int. J. Mech. Sci.* **41**, 235–248 (1999).
- <sup>17</sup> H. Wijshoff, "Free surface flow and acousto-elastic interaction in piezo inkjet," *Proc. Nanotechnol.* **2**, 215–218 (2004).
- <sup>18</sup> J. T. Youn and S. M. Lim, "Computer simulation of dot formation on paper in the gravure," *Korean Soc. Imaging Sci. Technol.* **14**, 62–70 (2008).
- <sup>19</sup> J. D. Yu, S. Sakai, and J. A. Sethian, "A coupled level set projection method applied to ink jet simulation," *Interfaces and Free Boundaries* **5**, 459–482 (2003). Downloaded from <http://math.berkeley.edu/~sethian/2006/Papers/sethian.inkjet.ifjb.2003.pdf>, 2/24/13.
- <sup>20</sup> J. D. Yu, S. Sakai, and J. A. Sethian, "A coupled quadrilateral grid level set projection method applied to ink jet simulation," *J. Comput. Phys.* **206**, 227–251 (2005).
- <sup>21</sup> H. Hu and G. R. Larson, *J. Phys. Chem. B* **106**, 1334–1344 (2002).
- <sup>22</sup> T.-M. Liou, C.-Y. Chan, and K.-C. Shin, "Effects of actuating waveform, ink property, and nozzle size on piezo electrically driven inkjet droplets," *Microfluid Nanofluid* (2009) DOI 10.1007/s10404-009-0488-4.
- <sup>23</sup> E. Ibrahim and A. Przekwas, "Impinging jets atomization," *Phys. Fluids A* **3**, 2981–2987 (1991).
- <sup>24</sup> T. Sayama and S. Yonekubo, "Device for driving inkjet print head," US Patent 6,074,033, (1998).